ROBUST HIGH-ORDER TENSOR RECOVERY VIA NONCONVEX LOW-RANK APPROXIMATION

Wenjin Qin[1], *Hailin Wang*[2], *Weijun Ma*[3], *Jianjun Wang*[1,*]

[1]School of Mathematics and Statistics, Southwest University, China
[2] School of Mathematics and Statistics, Xi'an Jiaotong University, China
[3] School of Information Engineering, Ningxia University, China

ABSTRACT

The latest tensor recovery methods based on tensor Singular Value Decomposition (t-SVD) mainly utilize the tensor nuclear norm (TNN) as a convex surrogate of the rank function. However, TNN minimization treats each rank component equally and tends to over-shrink the dominant ones, thereby usually leading to biased solutions. To handle this critical issue, we put forward a weighted tensor Schantten-p ($0 < p \leq 1$) norm (WTSN) as high-order tensor rank's more flexible nonconvex relaxation. Furthermore, another nonconvex ℓ_q ($0 < q \leq 1$) sparse regularization item on the extensively existed noises/outliers is incorporated into the WSTN minimization to enhance its robustness in the impulsive scenarios. Finally, we propose an efficient and scalable robust high-order tensor recovery method solving a double nonconvex optimization with convergence guarantees. Synthetic and real experiments demonstrate that the proposed approach outperforms the state-of-the-art ones in terms of both accuracy and computational complexity.

***Index Terms*—** Robust high-order tensor recovery, high-order randomized t-SVD, nonconvex low-rank approximation, nonconvex sparse regularization.

1. INTRODUCTION

Robust low-rank tensor recovery (RLRTR), which aims to recover the underlying low-rank tensor corrupted with sparse noise/outliers, is always an active topic in computer vision [1], signal processing [2], machine learning [3], etc. It can be viewed as a flexible extension of low-rank matrix recovery that is generally transformed into the rank minimization problem. Unlike the unique definition of matrix rank, however, the tensor rank has diversified forms owing to a greater variety of tensor decomposition schemes [4–9]. Among these decomposition strategies, the t-SVD has recently caught cumulative attention in various practical applications.

*✉ wjj@swu.edu.cn. This work is partially supported by National Natural Science Foundation of China under Grant Nos. 12071380, 62063028, and by the National Key Research and Development Program of China under Grant Nos. 2021YFB3101500.

Leveraging on the t-SVD framework, the multi-rank and tubal rank [10] were proposed to investigate the RLRTR problems related to third-order tensors. Since directly minimizing the tensor rank function results in an NP-hard problem, relevant researches substituted it for corresponding convex relaxation [11–14]. Most typically, Song et al. [14] proposed a novel transformed tensor nuclear norm (TNN) that is proved to be the convex envelope of the transformed tensor multi-rank within the unit ball of the transformed tensor spectral norm. Sequentially, they explored the model and algorithm for RLRTR via the proposed transformed TNN, and rigorously derived the theoretical guarantees for exact recovery.

Nevertheless, the transformed TNN is a loose approximation of the tensor rank function, which usually results in the over-penalization of the optimization problem and the sub-optimality of the obtained solution to the original problem. Besides, minimizing the transformed TNN would also cause some unavoidable biases in real applications. To fill the gaps resulted from the convex relaxation, some nonconvex surrogates induced from the transformed TNN were proposed to approximate the tensor rank function, e.g., weighted TNN [15], slice-weighted TNN [16], partial sum of TNN [17], tensor Schatten-p norm [18], tensor logarithmic norm [19]. Other researches concerning nonconvex relaxation can be found in [20, 21]. Although the above-mentioned nonconvex approaches induced by the t-SVD are efficient to some extent, we remark that these methods are only applicable to practical problems associated with third-order tensors.

With the tremendous advances in sensorial and information technology, massive amounts of order-d ($d > 3$) tensors are commonly encountered in real-world applications, such as order-4 color videos, order-5 light field images, order-6 bidirectional texture function images. Despite the restoration problem concerning these high-dimensional data can be coped by the RLRTR methods mentioned earlier, they generally lead to structural destruction of the original data. Driven by these concerns, in this paper, we first propose a new definition of weighted tensor Schatten-p ($0 < p \leq 1$) norm (WTSN) based on the generic framework of high-order t-SVD. By employing the WTSN minimization along with ℓ_q ($0 < q \leq 1$) sparse regularization, we then develop effective and scalable

model and algorithm for robust high-order tensor recovery (RHOTR). Experiments on both synthetic and real tensor data demonstrate that the proposed algorithm reconstructs the low-rank structures embedded in high-order tensors with the higher precision over the popular competitive ones.

2. ROBUST ORDER-D TENSOR RECOVERY

Due to the page limitation, the algebraic framework for order-d t-SVD and related algorithms involved in this section are posted on the author's github: https://github.com/Qinwenjinswu/high-order-t-SVD.

2.1. Proposed Model

Within the algebraic framework of order-d t-SVD, we formally introduce the double nonconvex model for RHOTR, i.e.,

$$\min_{\mathcal{L},\mathcal{E}\in\mathbb{R}^{n_1\times\cdots\times n_d}} \|\mathcal{L}\|^p_{\mathcal{W},\mathcal{S}_p}+\lambda\|\mathcal{E}\|_q^q, \quad \text{s.t. } \mathbf{P}_\Omega(\mathcal{L}+\mathcal{E})=\mathbf{P}_\Omega(\mathcal{M}), \tag{1}$$

where λ is penalty parameter, $\mathbf{P}_\Omega(\cdot)$ represents a linear operator such that the entries in the observed set Ω are given while the remaining entries (i.e., in $\overline{\Omega}$) are zeros. $\|\mathcal{E}\|_q$ denotes the ℓ_q-norm of sparse tensor $\mathcal{E}$, while $\|\mathcal{L}\|_{\mathcal{W},\mathcal{S}_p}$ denotes the WTSN of underlying low-rank tensor $\mathcal{L}$.

2.2. Optimization Method

The alternating direction method of multipliers (ADMM) framework [22] is adopted to solve the proposed model (1). By adding an auxiliary variable $\mathcal{K}=\mathcal{L}+\mathcal{E}$, the nonconvex model (1) can be equivalently reformulated as follows:

$$\min_{\mathcal{L},\mathcal{E}\in\mathbb{R}^{n_1\times\cdots\times n_d}} \|\mathcal{L}\|^p_{\mathcal{W},\mathcal{S}_p}+\lambda\|\mathcal{E}\|_q^q, \quad \text{s.t. } \mathcal{L}+\mathcal{E}=\mathcal{K},\ \mathbf{P}_\Omega(\mathcal{K})=\mathbf{P}_\Omega(\mathcal{M}). \tag{2}$$

The augmented Lagrangian function of (2) is

$$\mathcal{F}(\mathcal{L},\mathcal{E},\mathcal{K},\mathcal{Y})=\|\mathcal{L}\|^p_{\mathcal{W},\mathcal{S}_p}+\lambda\|\mathcal{E}\|_q^q+\langle\mathcal{Y},\mathcal{L}+\mathcal{E}-\mathcal{K}\rangle+\beta/2\|\mathcal{L}+\mathcal{E}-\mathcal{K}\|_F^2, \tag{3}$$

where $\mathcal{Y}$ is the dual variable and β is the regularization parameter. The ADMM framework alternately updates each optimization variable until convergence. Let $\mathcal{D}:=\{\mathcal{K}\in\mathbb{R}^{n_1\times\cdots\times n_d}:\mathbf{P}_\Omega(\mathcal{K})=\mathbf{P}_\Omega(\mathcal{M})\}$. The iteration template of the ADMM at the $(k+1)$-th iteration is described as follows:

$$\mathcal{K}^{k+\frac{1}{2}}=\arg\min\nolimits_{\mathcal{K}\in\mathcal{D}}\left\{\mathcal{F}(\mathcal{L}^k,\mathcal{E}^k,\mathcal{K},\mathcal{Y}^k)\right\}, \tag{4}$$

$$\mathcal{L}^{k+1}=\arg\min_{\mathcal{L}}\left\{\mathcal{F}(\mathcal{L},\mathcal{E}^k,\mathcal{K}^{k+\frac{1}{2}},\mathcal{Y}^k)\right\}, \tag{5}$$

$$\mathcal{K}^{k+1}=\arg\min\nolimits_{\mathcal{K}\in\mathcal{D}}\left\{\mathcal{F}(\mathcal{L}^{k+1},\mathcal{E}^k,\mathcal{K},\mathcal{Y}^k)\right\}, \tag{6}$$

$$\mathcal{E}^{k+1}=\arg\min_{\mathcal{E}}\left\{\mathcal{F}(\mathcal{L}^{k+1},\mathcal{E},\mathcal{K}^{k+1},\mathcal{Y}^k)\right\}, \tag{7}$$

$$\mathcal{Y}^{k+1}=\mathcal{Y}^k+\beta^k(\mathcal{L}^{k+1}+\mathcal{E}^{k+1}-\mathcal{K}^{k+1}), \tag{8}$$

$$\beta^{k+1}=\min\left(\beta^{\max},\vartheta\beta^k\right), \tag{9}$$

Algorithm 1 Solve $\min_{\mathcal{X}}\tau\|\mathcal{X}\|^p_{\mathcal{W},\mathcal{S}_p}+\frac{1}{2}\|\mathcal{X}-\mathcal{A}\|_F^2$.

Input: $\mathcal{A}\in\mathbb{R}^{n_1\times\cdots\times n_d}$, $\tau>0$, weight parameter: $\mathcal{W}\in\mathbb{R}^{n_1\times\cdots\times n_d}$, truncation term: $k<\min(n_1,n_2)$, the number of GST and PowerMethod iteration: α,β, $0<p\le 1$, oversampling parameter: $l>0$, and corresponding matrices $\{\mathrm{U}_{n_i}\}_{i=3}^d$ of invertible linear transforms L.

1. Choose the rt-SVD or t-SVD strategy to decompose $\mathcal{A}$ into $\mathcal{U},\mathcal{S},\mathcal{V}$
   if select the rt-SVD scheme **then**
   $[\mathcal{U},\mathcal{S},\mathcal{V}]=$ rtsvd-L$(\mathcal{A},L,k,l,\beta)$;
   else if select the t-SVD scheme **then**
   $[\mathcal{U},\mathcal{S},\mathcal{V}]=$ tsvd-L$(\mathcal{A},L)$;
   end if
2. Compute the matrix slice of $\mathcal{C}_L$ by
   for $i_3\in\{1,\cdots,n_3\},\cdots,i_d\in\{1,\cdots,n_d\}$ **do**
   $\sigma=\mathrm{diag}\left(\mathcal{S}_L(:,:,i_3,\cdots,i_d)\right)$;
   $w=\mathrm{diag}\left(\mathcal{W}(:,:,i_3,\cdots,i_d)\right)$;
   $\mathcal{C}_L(:,:,i_3,\cdots,i_d)=\mathrm{diag}(\mathrm{GST}(\sigma,\tau w,p,\alpha))$;
   end for
3. Compute the result of inverse linear transform on $\mathcal{C}_L$
   $\mathcal{S}_{\mathcal{W},p,\tau}\leftarrow L^{-1}(\mathcal{C}_L)$;

Output: $\hat{\mathcal{X}}=\mathcal{U}*_L\mathcal{S}_{\mathcal{W},p,\tau}*_L\mathcal{V}^*$.

where ϑ is the step-length. Now we solve each subproblem explicitly in the ADMM.

Update $\mathcal{L}$ (low-rank component) The optimization subproblem (5) can be written as

$$\min_{\mathcal{L}}\left\|\mathcal{L}\right\|^p_{\mathcal{W}^k,\mathcal{S}_p}+\frac{\beta^k}{2}\left\|\mathcal{L}-\mathcal{K}^{k+\frac{1}{2}}+\mathcal{E}^k+\frac{\mathcal{Y}^k}{\beta^k}\right\|_F^2. \tag{10}$$

Let $\mathcal{G}^k=\mathcal{K}^{k+\frac{1}{2}}-\mathcal{E}^k-\mathcal{Y}^k/\beta^k$. The subproblem (10) can be efficiently solved in virtue of the generalized soft-thresholding (GST) algorithm [23,24] and the generic order-d randomized t-SVD (rt-SVD) scheme, see Algorithm 1.

Remark 2.1. *(**Update $\mathcal{W}$ via reweighting strategy**) The weight parameters $\mathcal{W}^k$ are designed to be*

$$\mathcal{W}^k(:,:,i_3,\cdots,i_d)=c/\left(\mathcal{Q}^k(:,:,i_3,\cdots,i_d)+\epsilon\right), \tag{11}$$

where $c>0$ is a positive constant, $\epsilon>0$ is a small nonnegative constant to avoid division by zero, and the entries on the diagonal of $\mathcal{Q}^k(:,:,i_3,\cdots,i_d)$ represent the singular values of $(\mathcal{G}^k)_L\left(:,:,i_3,\cdots,i_d\right)$. In such a reweighted technique, the sparsity is enhanced after each iteration and the new entries of updated $\mathcal{W}^k$ satisfy: $\mathcal{W}^k(m,m,i_3,\cdots,i_d)\ge\cdots\ge\mathcal{W}^k(1,1,i_3,\cdots,i_d)\ge 0$ $(m=\min(n_1,n_2))$, $\forall i_j\in\{1,\cdots,n_j\},j\in\{3,\cdots,d\}$.

Update $\mathcal{E}$ (sparse component) The optimization subproblem (7) can be written as

$$\min_{\mathcal{E}}\lambda\|\mathcal{E}\|_q^q+\frac{\beta^k}{2}\left\|\mathcal{E}-\mathcal{K}^{k+1}+\mathcal{L}^{k+1}+\frac{\mathcal{Y}^k}{\beta^k}\right\|_F^2. \tag{12}$$

The closed-form solution for subproblem (12) can be computed by $\mathrm{prox}_{\frac{\lambda}{\beta^k}}(\mathcal{K}^{k+1}-\mathcal{L}^{k+1}-\mathcal{Y}^k/\beta^k)$, where $\mathrm{prox}_\eta(\cdot)$ is the element-wise shrinkage operator:

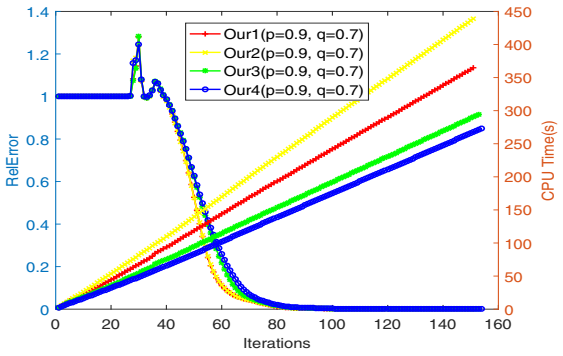

Fig. 1: Comparison of the relative error (fall) and CPU time (rise) versus iteration of the proposed algorithm on order-four synthetic tensor, where $n = 50, r = 10, sr = 0.7, \tau = 0.3$.

Table 1: Recovered results on synthetic order-four tensor.

n	r	m	$\|\mathcal{E}\|_0$	RelError$\mathcal{L}$			
				Ours1	Ours2	Ours3	Ours4
30	6	729000	145800	2.77e−8	2.49e−8	2.14e−8	2.26e−8
30	6	567000	113400	4.31e−8	4.26e−8	4.31e−8	4.51e−8
50	10	5625000	1125000	2.75e−8	2.69e−8	1.89e−8	2.29e−8
50	10	4375000	875000	4.24e−8	4.18e−8	4.59e−8	4.34e−8

$r = \text{rank}_{\text{tsvd}}(\mathcal{L}) = 0.2n,\ \|\mathcal{E}\|_0 = 0.2m\ \ (m = 0.9n^4, 0.7n^4)$

$$\text{prox}_\eta(x) = \begin{cases} 0, & \text{if } |x| < \delta, \\ \{0, \text{sign}(x)\hat{\alpha}\} & \text{if } |x| = \delta, \\ \text{sign}(x)\hat{\alpha}^* & \text{if } |x| > \delta. \end{cases} \tag{13}$$

In equation (13), $\hat{\alpha} = [2\eta(1-q)]^{\frac{1}{2-q}}$, $\delta = \hat{\alpha} + \eta q \hat{\alpha}^{q-1}$, and $\hat{\alpha}^*$ is the largest solution of $\alpha + \eta q \alpha^{q-1} = |x|$, where $\alpha > 0$. $\hat{\alpha}^*$ can be obtained from the iteration $\alpha_{(t+1)} = |x| - \eta q \alpha_{(t)}^{q-1}$ with the initial value $\alpha_{(0)} \in (\hat{\alpha}, |x|)$.

Update $\mathcal{K}$ (auxiliary variable) The closed-form solution with respect to $\mathcal{K}$ can be obtained through the standard least square regression method, i.e.,

$$\mathcal{K}^{k+\frac{1}{2}} = \mathbf{P}_\Omega(\mathcal{M}) + \mathbf{P}_{\overline{\Omega}}(\mathcal{L}^k + \mathcal{E}^k + \mathcal{Y}^k/\beta^k), \tag{14}$$

$$\mathcal{K}^{k+1} = \mathbf{P}_\Omega(\mathcal{M}) + \mathbf{P}_{\overline{\Omega}}(\mathcal{L}^{k+1} + \mathcal{E}^k + \mathcal{Y}^k/\beta^k). \tag{15}$$

2.3. Complexity Analysis

The main cost of Algorithm 2 is to update $\mathcal{L}$. For any invertible linear transforms L, the main cost of Algorithm 2 using rt-SVD/t-SVD is $\mathcal{O}(\prod_{i=1}^d n_i \cdot \prod_{j=3}^d n_j + k \cdot \prod_{k=1}^d n_k)$ / $\mathcal{O}(\prod_{i=1}^d n_i \cdot \prod_{j=3}^d n_j + \min\{n_1, n_2\} \cdot \prod_{k=1}^d n_k)$. For some special invertible linear transforms L, e.g., FFT, the main complexity of Algorithm 2 using rt-SVD/t-SVD is $\mathcal{O}(\prod_{i=1}^d n_i \cdot \log(\prod_{j=3}^d n_j) + k \cdot \prod_{k=1}^d n_k)$ / $\mathcal{O}(\prod_{i=1}^d n_i \cdot \log(\prod_{j=3}^d n_j) + \cdot \min\{n_1, n_2\} \cdot \prod_{k=1}^d n_k)$. RHOTR algorithm using rt-SVD technique can be advantageous when $k \ll \min\{n_1, n_2\}$.

Algorithm 2 Robust High-Order Tensor Recovery (RHOTR).

Input: Observed tensor: $\mathcal{M} \in \mathbb{R}^{n_1 \times \cdots \times n_d}$, observed index set: $\Omega \in \mathbb{R}^{n_1 \times \cdots \times n_d}$, penalty parameter: λ, invertible linear transform L, $0 < p \leq 1$, $0 < q \leq 1$, c, ϵ.
Initialize: $\mathcal{L}^0 = \mathcal{E}^0 = \mathcal{Y}^0 = \mathbf{0}$, $\vartheta > 1$, $\beta^0 = 10^{-3}$, $\beta^{\max} = 10^8$, $\varpi > 0$, $k = 0$.
while not converged **do**

1. Update $\mathcal{K}^{k+\frac{1}{2}}$ by computing (14);
2. Update $\mathcal{L}^{k+1}$ by computing (10);
3. Update $\mathcal{K}^{k+1}$ by computing (15);
4. Update $\mathcal{E}^{k+1}$ by computing (12);
5. Update $\mathcal{Y}^{k+1}$ by computing (8);
6. Update β^{k+1} by computing (9);
7. Check the convergence conditions

$\|\mathcal{L}^{k+1} - \mathcal{L}^k\|_F^2 / \|\mathcal{L}^k\|_F^2 \leq \varpi,\ \|\mathcal{E}^{k+1} - \mathcal{E}^k\|_F^2 / \|\mathcal{E}^k\|_F^2 \leq \varpi,$
$\|\mathcal{K}^{k+1} - \mathcal{L}^{k+1} - \mathcal{E}^{k+1}\|_F^2 / \|\mathcal{K}^k\|_F^2 \leq \varpi.$

end while

2.4. Convergence Analysis

Theorem 2.1. *If the diagonal elements of all matrix slices $\mathcal{W}(:,:,i_3,\cdots,i_d)$ on weighted tensor $\mathcal{W}^{k+1}$ are sorted in a non-descending order, then the sequences $\{\mathcal{L}^{k+1}\}$ and $\{\mathcal{E}^{k+1}\}$ generated by Algorithm 2 satisfy:*

1) $\lim_{k\to\infty} \|\mathcal{L}^{k+1} - \mathcal{L}^k\|_F = 0$; 2) $\lim_{k\to\infty} \|\mathcal{E}^{k+1} - \mathcal{E}^k\|_F = 0$;
3) $\lim_{k\to\infty} \|\mathcal{K}^{k+1} - \mathcal{L}^{k+1} - \mathcal{E}^{k+1}\|_F = 0$.

3. EXPERIMENTAL RESULTS

The variants of Algorithm 2 are induced by the combination of different invertible linear transforms L and two decomposition schemes. For brevity, four selected combinations "FFT + t-SVD", "DCT + t-SVD", "FFT + rt-SVD", "DCT + rt-SVD" are respectively called ours1, ours2, ours3, and ours4 in our experiment. All the experiments are implemented on the platform of Windows 10 and Matlab (R2016a) with an Intel(R) Xeon(R) Gold-6240 2.60GHz CPU and 64GB memory.

3.1. Robust Recovery of Synthetic Tensor

In this part, we conduct the robust low-rank tensor recovery on synthetic order-d data. The ground-truth low t-SVD rank tensor $\mathcal{L}$ with $\text{rank}_{tsvd}(\mathcal{L}) = r$ is generated by performing the order-d t-product $\mathcal{L} = \mathcal{L}_1 *_L \mathcal{L}_2$, where the entries of $\mathcal{L}_1 \in \mathbb{R}^{n \times r \times n \times \cdots \times n}$ and $\mathcal{L}_2 \in \mathbb{R}^{r \times n \times n \times \cdots \times n}$ are independently sampled from the normal distribution $\mathcal{N}(0, 1/n)$. Two linear transforms L are adopted: (a) Fast Fourier Transforms (FFT); (b) Discrete Cosine Transforms (DCT). Suppose that Ω is the observed index set while $\overline{\Omega}$ is the unobserved index set. Then, the construction of the sparse tensor $\mathcal{E} \in \mathbb{R}^{n \times \cdots \times n}$ with sparsity degrees τ satisfies as follows: 1) the elements

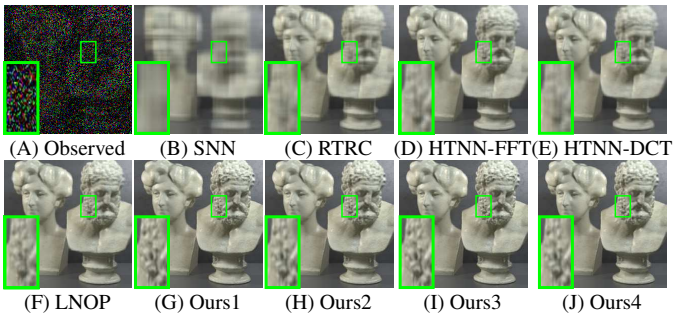

Fig. 2: Visual comparison of various methods for LFI restoration when $sr = 0.25, \tau = 0.3$.

of tensor $\boldsymbol{\mathcal{E}}$ in the unobserved index set $\overline{\Omega}$ are all equal to 0, i.e., $\mathbf{P}_{\overline{\Omega}}(\boldsymbol{\mathcal{E}}) = \mathbf{0}$; 2) each entry of tensor $\boldsymbol{\mathcal{E}}$ in the observed index set Ω takes on value 0 with probability $1-\tau$, and values $\{\pm 1\}$ each with probability $\tau/2$. Finally, we randomly sample $m = sr \cdot n^d$ elements from noisy tensor $\boldsymbol{\mathcal{L}} + \boldsymbol{\mathcal{E}}$ to construct the observed tensor, i.e., $\boldsymbol{\mathcal{M}} = \mathbf{P}_{\Omega}(\boldsymbol{\mathcal{L}} + \boldsymbol{\mathcal{E}})$. We evaluate the recovery performance by the Relative Error (RelError) defined as $\text{RelError}\boldsymbol{\mathcal{L}} := \|\hat{\boldsymbol{\mathcal{L}}} - \boldsymbol{\mathcal{L}}\|_F / \|\boldsymbol{\mathcal{L}}\|_F$, where $\hat{\boldsymbol{\mathcal{L}}}$ denotes the estimated result of the ground-truth $\boldsymbol{\mathcal{L}}$.

Table 1 reports the recovered result of the proposed algorithm (p=0.9, q=0.7) on synthetic order-four tensor, where the RelError values are very small (less than 10^{-7}) in all experimental scenes. As plotted in Figure 1, the proposed method reaches a relatively stable and small RelError value after about 80 iterations. More importantly, the RHOTR methods using rt-SVD method yields the lower computational cost than the ones without rt-SVD scheme.

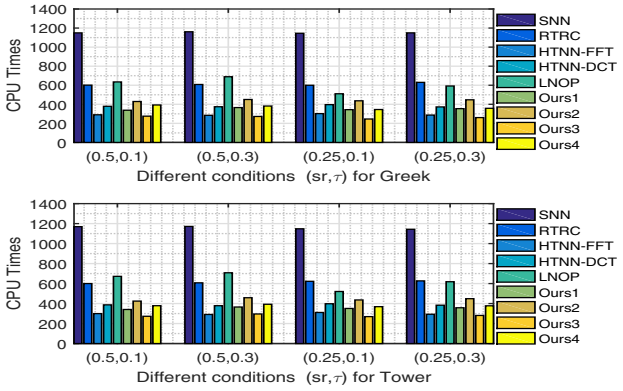

Fig. 3: Comparison of CPU times for LFIs restoration.

3.2. Application to Light Field Images Restoration

This subsection chooses two fifth-order light field images (LFIs[1]) including Greek and Tower to further show the superiority and effectiveness of the proposed RHOTR algorithm. To improve the computational time, we reshape the original

[1] https://lightfield-analysis.uni-konstanz.de/

Table 2: The PSNR value (db) of various methods for LFI.

LFI-Name	Greek				Tower			
sr	50%		25%		50%		25%	
τ	10%	30%	10%	30%	10%	30%	10%	30%
SNN	28.95	23.93	24.17	20.74	29.27	25.53	25.16	22.12
RTRC	39.05	31.24	32.23	27.31	37.49	31.06	31.82	27.69
LNOP	37.32	32.06	33.14	28.71	36.75	32.59	33.05	29.13
HTNN-FFT	35.11	30.91	30.73	27.59	35.33	31.33	31.16	28.14
HTNN-DCT	34.76	30.17	30.55	27.21	34.49	30.01	30.38	26.94
Ours1	44.61	40.69	36.36	33.45	40.47	37.07	34.92	32.81
Ours2	**48.29**	**43.62**	**38.74**	**35.34**	**42.21**	**38.37**	**36.08**	**33.78**
Ours3	43.94	39.19	36.07	33.36	40.04	36.99	34.91	32.79
Ours4	47.86	41.84	38.41	35.25	41.21	38.15	36.03	33.77

LFIs with the size of $512 \times 512 \times 3 \times 9 \times 9$ to be the ones with the size of $256 \times 256 \times 3 \times 9 \times 9$. The observed LFIs is generated as follows: the pepper-and-salt noise with ratio τ is added to the clean LFIs, and then $m = sr \cdot 256 \cdot 256 \cdot 3 \cdot 9 \cdot 9$ pixels are randomly sampled to form the observations. We apply the proposed method to restore these LFIs, and also compare our approach (p=0.9, q=0.7) with SNN [25], RTRC [26], TTNN-FFT [14], TTNN-DCT [14] and LNOP [19], where the last three modes of LFIs are combined into one mode for the third-order t-SVD based competing algorithms. The restoration performance is evaluated by the commonly-used peak signal-to-noise ratio (PSNR).

As listed in Table 2, the proposed method achieves the highest PSNR values than the state-of-the-art ones in all experimental scenes. It is observed that our method significantly improves the PSNR value of at least 3dB compared with the classical algorithms based on third-order t-SVD in salt-and-pepper noise. Apart from quantitative assessment, the visual comparisons on the $(6, 6)$-th frame of Greek are also exhibited in Figure 2. We find that our method achieve the reasonable balance between denoising and detail retention, which verifies the effectiveness of the WTSN minimization for low-rank approximation and the ℓ_q sparse penalty for outlier suppression. Finally, we report the CPU running time of various competing algorithms for LFIs restoration in Figure 3. As expected, RHOTR algorithm using rt-SVD scheme provide the superior computational efficiency.

4. CONCLUSION

Under the algebraic foundation of order-d t-SVD, the flexible model for RHOTR is investigated by utilizing nonconvex low-rank and sparse penalties. Based on the randomized t-SVD and generalized soft-thresholding scheme, we then propose an efficient and scalable algorithm with convergence guarantees to solve it. Experiments on both synthetic and real-world data show that our method is capable of reconstructing the low-rank structure of tensors with the better accuracy and robustness against several state-of-the-art methods.

5. REFERENCES

[1] J. Hou, F. Zhang, H. Qiu, J. Wang, Y. Wang, and D. Meng, "Robust low-tubal-rank tensor recovery from binary measurements," *IEEE TPAMI*, 2021, doi:10.1109/TPAMI.2021.3063527.

[2] A. Wang, G. Zhou, Z. Jin, and Q. Zhao, "Tensor recovery via $*_L$-spectral k-support norm," *IEEE JSTSP*, vol. 15, no. 3, pp. 522–534, 2021.

[3] H. Kong, C. Lu, and Z. Lin, "Tensor Q-rank: new data dependent definition of tensor rank," *Mach. Learn.*, pp. 1–34, 2021.

[4] R. A. Harshman, "Foundations of the PARAFAC procedure: Models and conditions for an "explanatory" multimodal factor analysis," *UCLA Work. Papers Phonetics*, vol. 16, pp. 1–84, 1970.

[5] L. R. Tucker, "Some mathematical notes on three-mode factor analysis," *Psychometrika*, vol. 31, no. 3, pp. 279–311, 1966.

[6] I. V. Oseledets, "Tensor-train decomposition," *SIAM J. Sci. Comput.*, vol. 33, no. 5, pp. 2295–2317, 2011.

[7] M. E. Kilmer and C. D. Martin, "Factorization strategies for third-order tensors," *Linear Alg. Appl.*, vol. 435, no. 3, pp. 641–658, 2011.

[8] C. D. Martin, R. Shafer, and B. LaRue, "An order-p tensor factorization with applications in imaging," *SIAM J. Sci. Comput.*, vol. 35, no. 1, pp. A474–A490, 2013.

[9] Q. Zhao, G. Zhou, S. Xie, L. Zhang, and A. Cichocki, "Tensor ring decomposition," *arXiv preprint arXiv:1606.05535*, 2016.

[10] M. E. Kilmer, K. Braman, N. Hao, and R. C. Hoover, "Third-order tensors as operators on matrices: A theoretical and computational framework with applications in imaging," *SIAM J. Matrix Anal. Appl.*, vol. 34, no. 1, pp. 148–172, 2013.

[11] O. Semerci, N. Hao, M. E. Kilmer, and E. L. Miller, "Tensor-based formulation and nuclear norm regularization for multienergy computed tomography," *IEEE TIP*, vol. 23, no. 4, pp. 1678–1693, 2014.

[12] C. Lu, J. Feng, Y. Chen, W. Liu, Z. Lin, and S. Yan, "Tensor robust principal component analysis with a new tensor nuclear norm," *IEEE TPAMI*, vol. 42, no. 4, pp. 925–938, 2019.

[13] Q. Jiang and M. Ng, "Robust low-tubal-rank tensor completion via convex optimization." in *IJCAI*, 2019, pp. 2649–2655.

[14] G. Song, M. K. Ng, and X. Zhang, "Robust tensor completion using transformed tensor singular value decomposition," *Numer. Linear Algebr. Appl.*, vol. 27, no. 3, p. e2299, 2020.

[15] Y. Mu, P. Wang, L. Lu, X. Zhang, and L. Qi, "Weighted tensor nuclear norm minimization for tensor completion using tensor-svd," *Pattern Recognit. Lett.*, vol. 130, pp. 4–11, 2020.

[16] A. Wang, X. Song, X. Wu, Z. Lai, and Z. Jin, "Robust low-tubal-rank tensor completion," in *ICASSP*. IEEE, 2019, pp. 3432–3436.

[17] T.-X. Jiang, T.-Z. Huang, X.-L. Zhao, and L.-J. Deng, "Multi-dimensional imaging data recovery via minimizing the partial sum of tubal nuclear norm," *J. Comput. Appl. Math.*, vol. 372, p. 112680, 2020.

[18] H. Kong, X. Xie, and Z. Lin, "t-schatten-p norm for low-rank tensor recovery," *IEEE JSTSP*, vol. 12, no. 6, pp. 1405–1419, 2018.

[19] L. Chen, X. Jiang, X. Liu, and Z. Zhou, "Robust low-rank tensor recovery via nonconvex singular value minimization," *IEEE TIP*, vol. 29, pp. 9044–9059, 2020.

[20] H. Wang, F. Zhang, J. Wang, T. Huang, J. Huang, and X. Liu, "Generalized nonconvex approach for low-tubal-rank tensor recovery," *IEEE TNNLS*, 2021, doi:10.1109/TNNLS.2021.3051650.

[21] D. Qiu, M. Bai, M. K. Ng, and X. Zhang, "Nonlocal robust tensor recovery with nonconvex regularization," *Inverse Problems*, vol. 37, no. 3, p. 035001, 2021.

[22] S. Boyd, N. Parikh, and E. Chu, "Distributed optimization and statistical learning via the alternating direction method of multipliers," *Found. Trends Mach. Learn.*, vol. 3, no. 1, pp. 1–122, 2011.

[23] W. Zuo, D. Meng, L. Zhang, X. Feng, and D. Zhang, "A generalized iterated shrinkage algorithm for non-convex sparse coding," in *ICCV*, 2013, pp. 217–224.

[24] Y. Xie, S. Gu, Y. Liu, W. Zuo, W. Zhang, and L. Zhang, "Weighted schatten p-norm minimization for image denoising and background subtraction," *IEEE TIP*, vol. 25, no. 10, pp. 4842–4857, 2016.

[25] D. Goldfarb and Z. Qin, "Robust low-rank tensor recovery: Models and algorithms," *SIAM J. Matrix Anal. Appl.*, vol. 35, no. 1, pp. 225–253, 2014.

[26] H. Huang, Y. Liu, Z. Long, and C. Zhu, "Robust low-rank tensor ring completion," *IEEE TCI*, vol. 6, pp. 1117–1126, 2020.